Optical Detection of Ballistic Electrons Injected by a Scanning-Tunneling Microscope

M. Kemerink,[1] K. Sauthoff,[2] P. M. Koenraad,[1] J. W. Gerritsen,[3] H. van Kempen,[3] and J. H. Wolter[1]
[1]*COBRA Inter-University Research Institute, Eindhoven University of Technology, P.O. Box 513, 5600 MB Eindhoven, The Netherlands*
[2]*IV. Physikalisches Institut, Universität Göttingen, Bunsenstraße 13, D-37073 Göttingen, Germany*
[3]*Research Institute for Materials, University of Nijmegen, Toernooiveld, 6525 ED Nijmegen, The Netherlands*
(Received 25 September 2000)

We demonstrate a spectroscopic technique which is based on ballistic injection of minority carriers from the tip of a scanning-tunneling microscope into a semiconductor heterostructure. By analyzing the resulting electroluminescence spectrum as a function of tip-sample bias, both the injection barrier height and the carrier scattering rate in the semiconductor can be determined. This technique is complementary to ballistic electron emission spectroscopy since minority instead of majority carriers are injected, which give the opportunity to study the carrier trajectory after injection.

DOI: 10.1103/PhysRevLett.86.2404 PACS numbers: 73.40.Gk, 68.37.Ef, 73.50.Gr, 78.60.Fi

During the past two decades, scanning-tunneling microscopy (STM) and scanning-tunneling spectroscopy (STS) have proven their value as a tool for studying semiconductor structures with extreme spatial resolution. The main strength of both STM and STS, being an extreme sensitivity to surface properties, can also be regarded as a weakness if one is interested in buried structures. However, by measuring the ballistic current from an STM tip through a metallic surface layer, Bell and Kaiser were able to determine the height of a buried Schottky barrier [1]. This technique was coined ballistic electron emission spectroscopy (BEES). Since then, BEES has been used for the study of, among others, Schottky barriers [2], resonant states in double barrier structures [3], superlattice minibands [4], CuPt-type ordering [5], and quantum dots [6]. Nevertheless, one of the main technical problems in a BEES experiment remains the detection of the ballistically injected current. More importantly, due to the electrical detection scheme, it is extremely hard to obtain information about the carrier dynamics after it has passed the injection barrier, since any injected carrier contributes to the current, independent of the path followed after injection.

Taking the above into account, it is worthwhile to consider the use of optical methods for detecting the ballistic current. Apart from the order of magnitude in sensitivity that can be gained [7], using an optical detection method opens the possibility to follow the ballistic electron current perpendicular to the sample surface. By placing different optically active layers at various depths in the sample, the (differences in the) bias dependence of the corresponding peaks in the electroluminescence (EL) spectrum can be used to gain insight in the scattering and trapping of the carriers after injection. This will be illustrated below.

It should be noted that, in order to detect the injected current optically, one has to inject minority carriers [8] instead of majority carriers, as is done in BEES. The "optical detection of ballistic electrons" (ODBE) technique, proposed in this Letter, should therefore be regarded as complementary to BEES. More specifically, we will demonstrate the use of ODBE as a very promising spectroscopic technique for the study of buried heterostructures.

In general, three functional layers can be discerned in a BEES sample: first, a metallic base layer which collects the majority of the tunneling current and screens the deeper layers from the electric field between tip and sample; second, the layer determining the transmission, which in BEES is usually a Schottky barrier; and third, the collector region. Since ODBE requires the injection of minority carriers, the tip-sample bias U_t is such that an accumulation layer is formed at the surface for sufficiently large U_t. It has been shown that such an accumulation layer effectively screens the electric field [9]. Consequently, no separate metallic base layer is needed, and an all-semiconductor sample can be used. Omitting the metal top layer is advantageous, since it will raise the injected current because of the much longer attenuation length in semiconductors than in metals [10]. In principle, radiative recombination of the injected minority carriers in doped bulk material can be used as the optical detector in ODBE, but the use of a quantum well (QW) as an optical detector has several advantages. First, the luminescence efficiency ε_q of a typical QW is a few orders of magnitude larger than the ε_q of bulk material. Second, in bulk electric fields can lead to a separation between holes and electrons. This is especially the case for the situation where minority carriers are injected through a Schottky contact. The depletion field is then such that the minority carriers are driven towards the metal gate, away from the majority carriers. Third, one does not use the full potential of ODBE in terms of depth resolution.

The samples that were used in the ODBE experiments were grown by molecular beam epitaxy and contain, starting at the semi-insulating GaAs substrate, a 500 Å GaAs buffer layer, a 25-period GaAs/AlAs (50 Å/50 Å) superlattice (SL), a 450 Å $Al_{0.25}Ga_{0.75}As$ barrier layer, an $In_xGa_{1-x}As$ QW, again a 450 Å $Al_{0.25}Ga_{0.75}As$ barrier layer, and, finally, a 170 Å GaAs capping layer.

 0031-9007/01/86(11)/2404(4)$15.00 © 2001 The American Physical Society

Both barrier layers contain, at 250 Å from the QW, a Be delta-doping layer with a nominal density of 1×10^{12} cm^{-2}. All layers are unintentionally p-type doped at 1×10^{15} cm^{-3}. ODBE spectroscopy experiments were performed on samples cut from wafers with various indium contents and varying well width. Qualitatively, all wafers gave similar results, so only a single one, W661, will be discussed here as a typical example. W661 has a well width of 83 Å and the indium context $x = 0.10$. Figure 1 shows a self-consistent band diagram of W661 for a tip-sample bias U_t of 1.91 V. Note that the sample surface is a 001 plane, i.e., the tip axis is aligned along the growth direction. The screening of U_t by the formation of a surface accumulation layer is illustrated in the inset of Fig. 1. Plotted are the conduction band energies at the surface (marked A) and at the middle of the first AlGaAs barrier (B). After the formation of the hole accumulation layer, i.e., for $U_t > 0$ V, the band energies below the capping layer are fully independent of bias, due to the screening by the accumulation layer.

Since the samples are mounted under ambient conditions, the following passivation procedure was used. First, the samples are etched in diluted HCl for 30 s. Immediately afterwards, they are plunged into a saturated solution of Na_2S in isopropanol. After 2 min, they are removed from the solution, flushed with distilled water, and blown dry with nitrogen. The last step consists of a 10 min anneal at 400 °C under a protective atmosphere. This procedure results in a sample surface that is covered with one and a half monolayers of Ga-bound S [11], that is free of gap states [12] and that we found to be stable against oxidation for at least several weeks.

After passivation, the samples were mounted in the head of a home-built low-temperature STM. The STM can be operated in temperatures down to approximately 2 K and in magnetic fields up to 11 T. The tunneling tips were etched from 0.15 mm polycrystalline platinum wire [13]. The STM is contained by a stainless steel tube that is filled with high-purity He gas, which provides both an inert environment and thermal contact to the liquid-He bath. Optical access is accomplished by means of two fibers with a core diameter of 0.60 mm, of which the cleaved end is positioned close to the tunneling region. The collected light is dispersed by a 30 cm monochromator and detected by a cooled Si charge-coupled device (CCD) camera. Typical integration times are 1–2 min at room temperature and 0.5–1 min at low (4.2/77 K) temperatures, giving rise to an integrated intensity of the order of 10^4 and 10^6 counts/min, respectively, at $U_t = 3.5$ V and $I_t = 10$ nA. More details about the used setup will be given in a forthcoming publication [14].

Although the maximum applied currents and biases were rather high, no indication of surface damage was found in the simultaneously taken topography. In principle, the discussed technique can also be used for spatially resolved measurements. However, because of the relatively long integration times needed, no such measurements are performed on these samples.

An example of a low-temperature ODBE spectrum is displayed in the inset of Fig. 2. From the integrated intensity, we estimate the total conversion efficiency ε_t, i.e., the number of photons created in the QW per electron emitted by the STM tip, to be 7×10^{-4} at $T = 4.2$ K and $U_t = 3.5$ V. The relatively low value found for ε_t is most likely due to nonradiative recombination at surface states. I-V calculations performed along the lines of Feenstra and Stroscio [15] show that the fraction of the current that is injected in the valance band is negligible at the used biases. The dependence of the EL intensity on the applied bias is shown in the main panel of Fig. 2. To

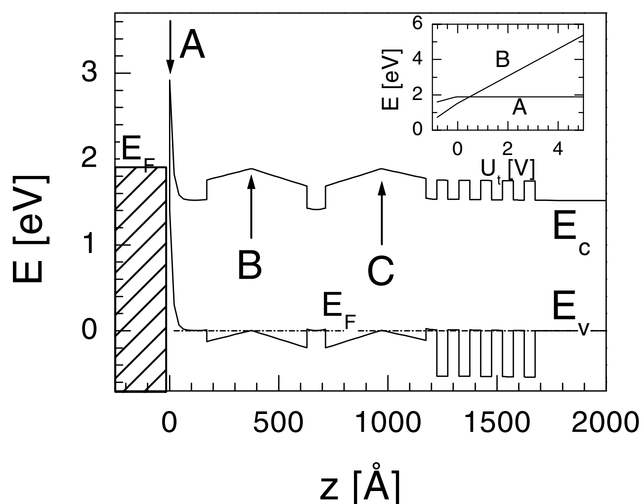

FIG. 1. Self-consistent band diagram of W661 for $U_t = 1.91$ V and a tip-sample gap of 8 Å. Inset: Conduction band energy at the points marked A and B versus U_t, showing the screening by the surface accumulation layer.

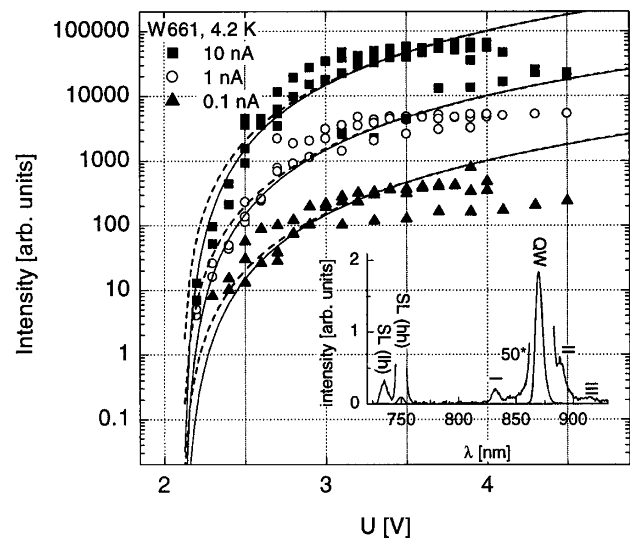

FIG. 2. Bias dependence of the QW-EL intensity at $I_t = 10$, 1.0, and 0.10 nA. Inset: Full EL spectrum at $I_t = 10$ nA and $U_t = 3.5$ V.

interpret the bias dependence, an extension has to be made to the conventional BEES model to account for the scattering of the injected carriers. Prior to recombination in the QW, an electron has, after transmission over the first AlGaAs barrier, to relax to the bottom of the conduction band, $E_{c,0}$. However, electrons that reach $E_{c,0}$ before the first doping δ-layer (B in Fig. 1) or after the second δ-layer (C) are driven away from the QW region by the electric field and will not contribute to the ODBE signal from the QW. The other carriers, i.e., those that reach $E_{c,0}$ between B and C, will be driven to the QW by the built-in fields and contribute to the ODBE signal. For recombination in the SL, a similar argument holds. By assuming that the injected electrons, with group velocity ν, are scattered with rate Γ_s, we find the following for the number of unscattered (ballistic) electrons n_b as a function of depth:

$$\frac{dn_b(E,\mathbf{k})}{dz} = \frac{dn_b(E,\mathbf{k})}{dt}\frac{dt}{dz} = -\frac{n_b(E,\mathbf{k})\Gamma_s(E,\mathbf{k})}{\nu(E,\mathbf{k})}. \quad (1)$$

Since no effects of injection in higher subbands are observed, we limit our modeling to an single conduction band. Moreover, we assume that the conduction band is characterized by an effective mass m^*, and a scattering rate that is independent of energy. It is reasonable to assume that at the used injection energies the dominant scattering mechanism is LO-phonon scattering. Since LO-phonon scattering is isotropic, the direction of the electron is fully randomized after a single scattering event. Therefore, even if multiple scattering events are needed to relax to $E_{c,0}$, the distribution of depths at which $E_{c,0}$ is reached will be centered around the position of the first scattering event. So, to recombine in the QW, the *first* scattering event should, in lowest order, take place between the two δ-layers. Up to this point, the electron path is purely ballistic. Under the above conditions, we find the following for the number of electrons that reaches the QW:

$$L \propto I_t\left(\exp\left[-\frac{\sqrt{m^*/2}\,\Gamma_s z_B}{\sqrt{e(U_t - U_0)}}\right] - \exp\left[-\frac{\sqrt{m^*/2}\,\Gamma_s z_C}{\sqrt{e(U_t - U_0)}}\right]\right)[e(U_t - U_0)]^{2.5}, \quad (2)$$

where $z_{B,C}$ are the z values at positions B and C in Fig. 1, i.e., at the first and second δ-doping layer, U_0 is the height of the first barrier, and I_t is the tunneling current. The last term accounts for the voltage dependence due to k conservation and quantum-mechanical reflection at the first barrier, and is well-known from BEES theory [16]. The solid lines in Fig. 2 are fits to (2) with $U_0 = 2.1$ V and 5×10^{13} s^{-1}; the dashed lines are fits to the last term of Eq. (2) only, which is the usual BEES formula. The value found for U_0 is in reasonable agreement with the value obtained from the self-consistent calculation shown in Fig. 1, 1.9 V. From the fitted scattering rate Γ_s, we find for electrons with an excess energy of 0.1 eV, i.e., $U_t = 2.2$ V, a ballistic mean free path of 15 nm, which appears reasonable [10]. Of course, in our model the ballistic mean free path increases with the square root of the excess energy. From similar measurements at 77 K, we find $U_0 = 1.8$ V and $\Gamma_s = 8 \times 10^{13}$ s^{-1}, which yields a ballistic mean free path of 9 nm at 0.1 V excess energy. At room temperature, we find that the linearity of the ODBE signal with the tunneling current no longer holds due to an additional, nonradiative, recombination channel caused by electron traps, as has been reported previously [17]. The tentative assignment of the Be acceptors as trapping centers in Ref. [17] is further substantiated by the complete disappearance of the nonlinearity at 77 K. Since the electron binding energy to a Be acceptor is 30 meV [18], thermal excitation of trapped electrons is negligible at 77 K, so the current needed to saturate the nonradiative trap channel becomes negligible as well.

Obviously, the difference in Fig. 2 between the full model and the conventional BEES model is not very substantial, which is due to the fact that the majority of the injected electrons will recombine in the quantum well. Therefore the first term on the right-hand side of (2) becomes almost unity, and the relative change with U_t is small. The fraction of electrons that travel ballistically beyond the second doping layer and recombine radiatively in the superlattice is an order of magnitude lower, so the relative change with changing U_t in the first term of (2) becomes more pronounced. This is illustrated in the lower panel of Fig. 3, where the solid symbols show the voltage dependence of the intensity of the SL and QW lines in the EL spectrum. Clearly, the conventional BEES model yields a very poor description of the heavy (hh) and light (lh) hole superlattice peak data, for the reasons mentioned above. In contrast, the full model gives an excellent description of the data. It should be stressed that the lines corresponding to the SL electroluminescence are fitted with the same U_0 and Γ_s as are used for the QW. The difference in voltage dependence between the SL and QW signals is made more clear in the top panel of Fig. 3, which shows the intensity ratio of the various peaks in the electroluminescence spectrum and the QW peak. Again, the solid lines, which are simply generated by division of the corresponding curves in the lower panel, show an excellent agreement with the data. Obviously, the conventional BEES model yields a constant value for the intensity ratio, and has been omitted in the upper panel of Fig. 3. It is interesting to see that the small additional peaks around the QW peak, labeled I, II, and III in the inset of Fig. 2, have exactly the same voltage dependence as the QW itself. Therefore we can identify these peaks as originating from the QW. We attribute peaks II and III, that are redshifted by 31.9 and 70.4 meV with respect to the main QW peak, as phonon replicas of the main peak. The 66.9 meV blueshifted peak I is attributed to a transition from ground state light holes to ground state electrons. From self-consistent envelope function calculations, we expect a blueshift for this transition of 63.8 meV [19].

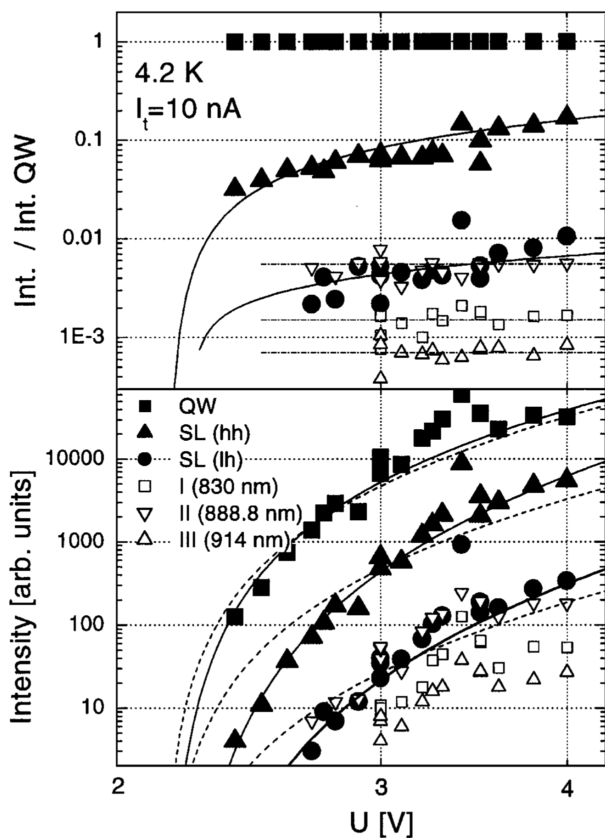

FIG. 3. Lower panel: Bias dependence of all EL peaks at $I_t = 10$ nA. The solid (dashed) lines are fits to the llllfull (conventional BEES) model. Upper panel: Intensity ratio of all EL peaks and the QW peak. The solid lines are fits to the full model; the dash-dotted lines guide the eye.

In our modeling, we implicitly assumed that the fraction of carriers that is transmitted through the passivated surface layer, $\varepsilon_{\rm surf}$, is independent of bias. The good correspondence between the fit to the model and the data confirms that this assumption is indeed reasonable. Using (2) and the measured total conversion efficiency ε_t, we find $\varepsilon_{\rm surf} = 6.6 \times 10^{-4}$. From (2), we calculate the fraction that recombines in the QW (SL) is 1.1×10^{-5} (1.5×10^{-6}) at 2.5 V, 1.4×10^{-4} (4.8×10^{-5}) at 3.0 V, and 4.6×10^{-4} (2.4×10^{-4}) at 3.5 V. Note that the ratio between the fractions recombining in the QW and SL decreases from 7.3 and 2.5 V to 1.9 at 3.5 V due to the increasing mean free path of the injected electrons.

In conclusion, we have demonstrated a novel spectroscopic technique, optical detection of ballistic electrons, based on the ballistic injection of minority carriers from a STM tip into a semiconductor heterostructure. By radiative recombination with majority carriers localized in optically active layers an EL spectrum is generated. Although ODBE can be regarded as the optical counterpart of, and complementary to, BEES, an extension to the conventional BEES theory had to be made to account for the relaxation of the injected carriers. In BEES, this is unimportant since the electrical detection scheme can tell only whether or not a carrier is injected, but not how the carrier relaxes after injection. By analyzing the distribution of the spectral intensity over the various recombination channels as a function of tip-sample bias, the carrier scattering rate in $Al_{0.25}Ga_{0.75}As$ could be determined to be 5×10^{13} s^{-1} at 4.2 K and 8×10^{13} s^{-1} at 77 K. From the same measurements, the injection barrier height could be determined.

The research of Dr. M. Kermerink has been made possible by a fellowship of the Royal Netherlands Academy of Arts and Sciences. One of the authors (K. S.) acknowledges financial support by the Deutsche Forschungsgemeinschaft (SFB 345). Furthermore, we gratefully acknowledge P. A. M. Nouwens and J. G. H. Hermsen for technical assistance.

---

[1] W. J. Kaiser and L. D. Bell, Phys. Rev. Lett. **60**, 1406 (1988).

[2] G. M. Vanalme *et al.,* Semicond. Sci. Technol. **14**, 871 (1999).

[3] T. Sajoto *et al.,* Phys. Rev. Lett. **74**, 3427 (1995).

[4] J. Smoliner, R. Heer, and G. Strasser, Phys. Rev. B **60**, 5137 (1999).

[5] M. Kozhevnikov *et al.,* Appl. Phys. Lett. **75**, 1128 (1999).

[6] M. E. Rubin *et al.,* Phys. Rev. Lett. **77**, 5268 (1996).

[7] We placed two 0.6 mm fibers at about 1.5 mm from the tunneling region, giving a photon collection efficiency of 8×10^{-4}. Since the quantum efficiency of the optically active layers is almost unity at 4.2 K, and the detection limit of our CCD is a few photons per second, we can optically detect an injected current of the order of 1 fA. Electronically, the detection limit is about 20 fA.

[8] In principle, minority carriers can be generated by impact ionization of majority carriers injected at high enough voltages. However, the used samples showed very poor tunneling behavior at the required biases.

[9] H.-A. Lin, R. J. Jaccodine, and M. S. Freund, Appl. Phys. Lett. **73**, 2462 (1998).

[10] R. Heer *et al.,* Appl. Phys. Lett. **73**, 1218 (1998).

[11] N. Yokoi *et al.,* Jpn. J. Appl. Phys. **33**, 7130 (1994).

[12] G. Hirsch, P. Krüger, and J. Pollmann, Surf. Sci. **402–404**, 778 (1998).

[13] L. Libioulle, Y. Houbion, and J.-M. Gilles, Rev. Sci. Instrum. **66**, 97 (1995).

[14] M. Kemerink *et al.,* Rev. Sci. Instrum. **72**, 132 (2001).

[15] R. M. Feenstra and J. A. Stroscio, J. Vac. Sci. Technol. B **5**, 923 (1987).

[16] M. Prietsch and R. Ludeke, Phys. Rev. Lett. **66**, 2511 (1991).

[17] M. Kemerink *et al.,* Appl. Phys. Lett. **75**, 3656 (1999).

[18] E. F. Schubert, in *Doping in III/V Semiconductors* (Cambridge University, Cambridge, England, 1994).

[19] M. Kemerink, P. M. Koenraad, and J. H. Wolter, Phys. Rev. B **54**, 10 644 (1996).